



Copper(I)-carbenes as key intermediates in the [3+2]-cyclization of pyridine derivatives with alkenyldiazoacetates: A computational study

Received 00th January 20xx,
Accepted 00th January 20xx

DOI: 10.1039/x0xx00000x

www.rsc.org/

Luis A. López,^{*a,b} and Javier González^{*a}

This work reports a computational study of the copper(I)-catalyzed regioselective synthesis of indolizine derivatives through [3+2]-cyclization reaction of vinyldiazo acetates and pyridine derivatives. This reaction is predicted to proceed by way of a multi-step process with initial decomposition of the diazo function and generation of an electrophilic copper(I) carbene intermediate. Subsequent attack of the pyridine derivative to the vinylogous position of the carbene would generate a vinylcuprate intermediate that would evolve to the final products through a sequence involving cyclization, reductive elimination, metal decoordination and final oxidative aromatization. According to our calculations, an alternative pathway involving initial activation of the pyridine seems unlikely. These theoretical results could pave the way for further developments in vinyldiazo chemistry.

Introduction

Although stabilized diazo compounds have been known and studied for many years, these reagents continue to play an important role in contemporary synthetic organic chemistry.¹ Stabilized vinyldiazo compounds are a subset of diazo reagents that have also developed into useful substrates in transition metal catalyzed transformations. The presence of two reactive conjugated functional groups (diazo and alkene) in their structure provides a rich chemistry that has been successfully exploited in many synthetically useful metal-catalyzed transformations.² In this regard, dirhodium catalysts have become particularly popular allowing the development of a wide variety of highly selective reactions.³ In most of these rhodium-catalyzed transformations, vinyldiazo reagents can serve as convenient precursors to donor/acceptor rhodium carbene species which evolve to the final products through carbenoid pathways (heteroatom-hydrogen and carbon-hydrogen insertions, cyclopropanation, ylide formation, cycloadditions, ...). Very recently, coinage metals have also become useful catalysts in transformations involving vinyldiazo compounds.⁴ In particular, the use of gold-based catalysts has been the focus of intense recent investigations allowing to identify new reactivity patterns in vinyldiazo chemistry, thus expanding the synthetic versatility of these diazo compounds.⁵

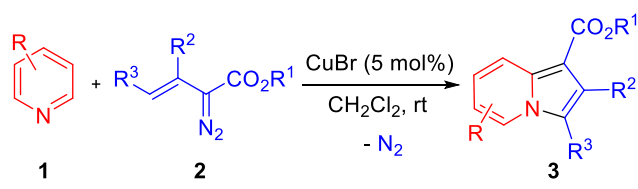
The multifunctional character of these diazo compounds is also the origin of some mechanistic intricacies and, not infrequently, different pathways can be proposed for the formation of a particular product. The copper-catalyzed [3+2] cyclization reaction of pyridine derivatives **1** and vinyldiazo compounds **2** reported some years ago by our research group is one such reaction for which different reaction courses could be envisioned for the regioselective formation of the final indolizine derivatives **3** (Scheme 1).⁶ Indeed, pyridine activation by Lewis acid complexation followed by nucleophilic attack of the diazo function and final cyclization would account for the regiochemical outcome. Prior to our work, Doyle and co-workers proposed a mechanism of this type for the formation of dihydropyrrole derivatives in the copper(II) triflate-catalyzed reaction of vinyldiazo compounds and some imine derivatives.⁷ Alternatively, decomposition of the diazo reagent with generation of an electrophilic copper carbene intermediate,⁸ followed by Michael type addition of the pyridine and final cyclization and oxidation steps would also account for the observed regioselectivity.

The aim of this contribution is to unravel this mechanistic intricacy and, eventually, to identify new and potentially useful patterns in vinyldiazo chemistry. To this purpose, we have performed a computational mechanistic study of both reaction pathways.

^a Departamento de Química Orgánica e Inorgánica, Universidad de Oviedo, Julián Clavería, 8, 33006 Oviedo, Spain. E-mail: lalq@uniovi.es, jjgf@uniovi.es

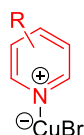
^b Instituto Universitario de Química OrganoMetalítica "Enrique Moles", Universidad de Oviedo

† Electronic Supplementary Information (ESI) available: Cartesian coordinates and energies of the stationary points located. See DOI: 10.1039/x0xx00000x



Potential roles of the catalyst

A) Activation of the pyridine partner



B) Activation of the diazo partner



Scheme 1. Copper(I)-catalyzed [3+2] cycloaddition reaction of pyridine derivatives **1** and vinyl diazo compounds **2**: Synthesis of indolizine derivatives **3**. Potential activation modes.

Computational methodology

The theoretical study of the CuBr-catalyzed [3+2]-cyclization of pyridine derivatives with alkenyldiazoacetates has been carried out with the pyridine derivatives **1a-e** (R = H, 3-Me, 3-NO₂, 3-CO₂Me and 3-F) and the alkenyldiazoacetate **2a** (R = Me; R² = Me; R³ = H) as model of the reactants (Figure 1).

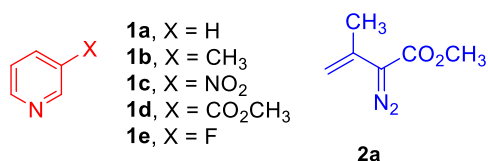


Figure 1. Substrates used in this theoretical study.

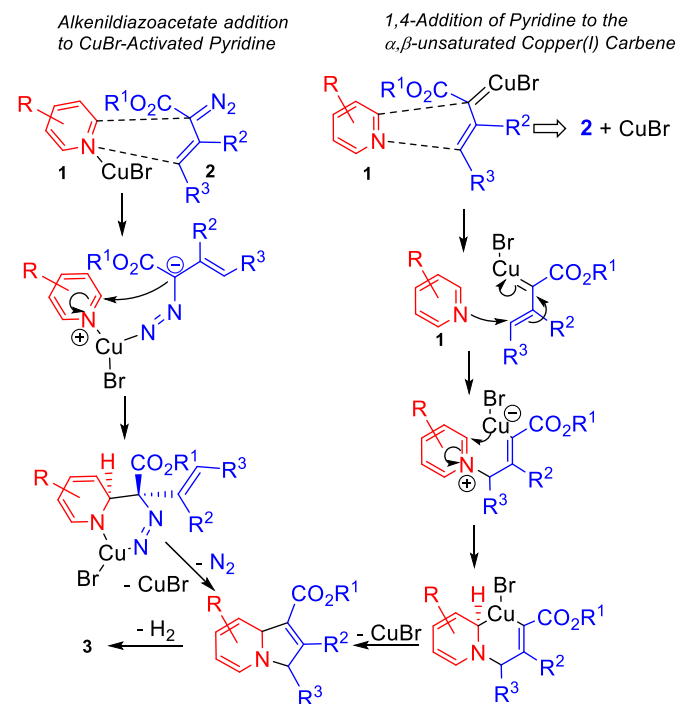
The potential energy surface of the reactions considered was studied with the density functional theory (DFT), using the hybrid functional B3LYP and the 6-31G(d) basis set. This level of theory has been shown to be adequate for the description of several catalytic systems.⁹ Additionally, calculations at B3LYP/6-311+G(d) and MP2/6-311+G(d) [using the 6-31G(d) basis set for copper and bromine atoms] levels of theory were carried out in the case of the reaction corresponding to the formation of copper(I) carbene intermediate.

The geometry of each stationary point located was fully optimized in all cases. Each stationary point was characterized to be a minimum or a first-order saddle point (transition structure) by computing the harmonic vibrational frequencies at 298.150 K and 1.0 atm. The connection of either, the reactants or products with the corresponding transition structure was established by computation of the intrinsic reaction coordinate (IRC). The Cartesian coordinates and energies of the stationary points located are collected in the ESI section.

The calculations described in this work were carried out with Gaussian03 and Gaussian09 suite of programs.¹⁰

Results and discussion

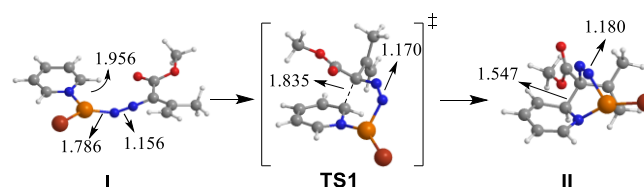
As stated before, two different mechanisms (see Scheme 2) for the reaction of pyridines with alkenyldiazoacetates, in the presence of CuBr as catalyst, may be envisaged, namely the direct addition of the diazo compound to the pyridine, activated by CuBr acting as a Lewis acid, or the conjugate addition of pyridine to an α,β -unsaturated copper(I) carbene intermediate, which is proposed to form in a reaction of the alkenyldiazoacetate with CuBr.



Scheme 2. Proposed mechanisms for the CuBr-catalyzed reaction of **1** with **2**.

Direct Addition of Diazocompound **2a** to CuBr-Activated Pyridine derivatives **1**

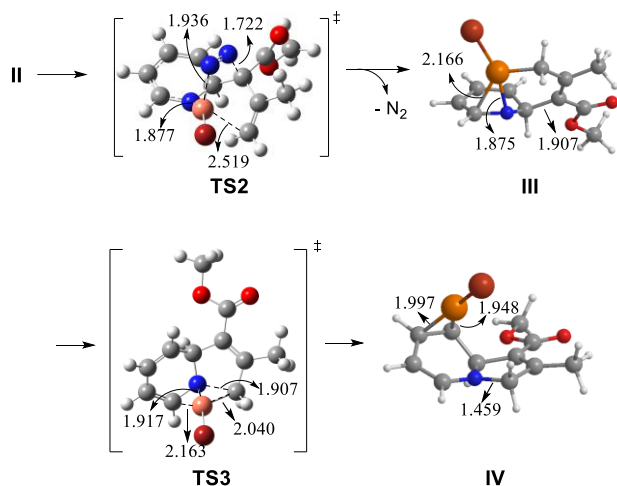
The potential-energy surface corresponding to the reaction of pyridine **1a** with CuBr and the diazo compound **2a** (Scheme 3), was first studied and several stationary points were located. **1a**, CuBr and **2a** form a complex **I**, which undergoes an intramolecular *ortho*-addition of the nucleophilic carbon atom, *via* transition structure **TS1**, leading to bicyclic intermediate **II**. The imaginary normal mode corresponding to **TS1** is associated to the bond-forming between the diazo carbon atom of **2a** to the C-2 of the pyridine ring.



Scheme 3. Stationary points corresponding to the reaction of **1a** with **2a** in presence of CuBr. Lengths are in Å.

Intermediate **II** is predicted to undergo extrusion of the dinitrogen molecule through the transition structure **TS2**,

leading to the metallacycle intermediate **III** (Scheme 4). Finally, reductive elimination of CuBr from metallacycle **III**, with a simultaneous formation of the carbon-carbon bond, *via* the transition structure **TS3**, leads to the indolizine derivative **IV**, in which the CuBr moiety is η^2 -coordinated to the pyridine ring.



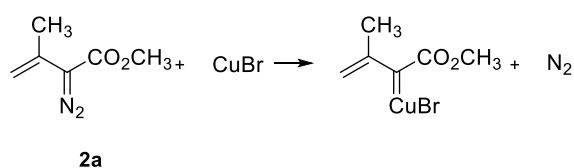
Scheme 4. Stationary points corresponding to the extrusion of dinitrogen and reductive elimination to form the η^2 -CuBr coordinated to the indolizine structure, **IV**. Lengths are in Å.

The mechanism just described explains the formation of the indolizine derivatives **3** and resembles the one proposed by Doyle and co-workers. However, the values of the predicted activation barriers for the intramolecular cyclization ($\Delta G^\ddagger = 43.8 \text{ kcal mol}^{-1}$) and dinitrogen extrusion ($\Delta G^\ddagger = 41.8 \text{ kcal mol}^{-1}$) are very high and appear to be incompatible with the reaction conditions experimentally found. In addition, this mechanism involving the direct addition of the alkenyldiazocompound **2** to pyridine derivatives **1**, incorrectly predicts the regioselectivity observed in the case of the reaction with 3-methylpyridine **1b** and 3-nitropyridine, **1c** (see ESI for full details).

Next, the alternative mechanism, depicted in Scheme 2 and involving a conjugate addition of pyridines **1** to a copper(I) carbene intermediate was investigated.

Copper(I) carbene formation by reaction of diazocompound **2a** with CuBr

In order to explain the formation of a copper(I) carbene intermediate (Scheme 5), the potential-energy surface corresponding to the reaction between **2** and CuBr, was explored in detail.



Scheme 5. Proposed reaction between **2a** and CuBr leading to α,β -unsaturated copper(I) carbene intermediate.

Several complexes between **2a** and CuBr, with different geometries and energies, were located in the potential-energy surface. All the structures found are shown in the ESI section. Here, only the most stable structure, **Va**, which is characterized by a η^2 -coordination of copper(I) to the double bond of **2a** is presented.

The most relevant structural details of complex **Va** are shown in Figure 2, together with those of diazocompound **2a**, for comparison. As can be seen, the π -coordination of copper(I) bromide to the C-C double bond of **2a** causes a slight increase (from 1.343 Å to 1.398 Å) of the length of the C-C double bond in **Va**, probably due to a retrodonation of electron density from copper to the antibonding orbitals of the diazocompound. In addition, upon coordination, the length of the Cu-Br bond, increases from 2.095 Å, in the free copper(I) bromide to 2.239 Å in complex **Va**. Also, in **2a**, the $\text{CH}_2\text{C}(\text{Me})$ and $\text{N}_2\text{C}(\text{CO}_2\text{Me})$ moieties are coplanar, whereas in **Va**, they are rotated about 90° , thus allowing the coordination of the carbonyl oxygen of the ester to the copper atom, which is reflected in the small distance between Cu and O atoms in **Va**. The formation of complex **Va** seems to be barrierless, and this structure is quite stabilized (about 60 kcal mol^{-1}) respect to **2a** and CuBr.

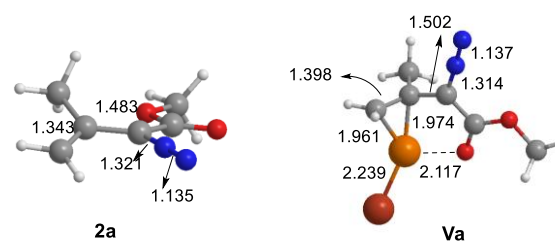
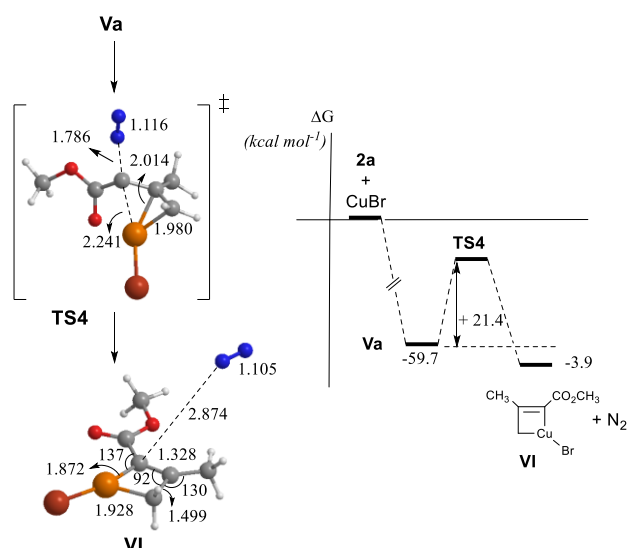


Figure 2. Selected geometrical details of diazocompound **2a** and complex **Va**. Lengths are in Å.

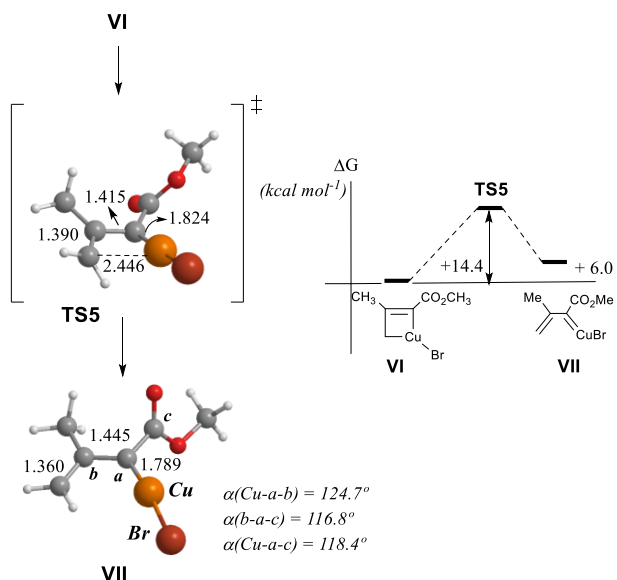
The formation of copper(I) carbene intermediate **VII** would take place through dinitrogen extrusion from complex **Va** which gives rise to the metallacyclobutene **VI** (Scheme 6).

The imaginary normal mode of transition structure **TS4** corresponds to the breaking of the bond C-N=N and the formation of the N_2 molecule, and to the Cu-C bond formation, so this process can be seen as a concerted [1,2]-shift of copper atom and N_2 extrusion. In intermediate **VI**, the dinitrogen molecule is far away (2.874 Å) from the metallacycle, and the NN triple bond is fully formed.



Scheme 6. Reaction pathway for the dinitrogen extrusion from complex **Va** and forming the C-Cu bond of copper cyclobutane intermediate **VI**. Lengths and angles are in Å and degrees, respectively.

The last step in the formation of the copper carbene intermediate **VII**, is the ring-opening of the metallacycle **VI**, in a formal electrocyclic ring-opening leading to the α,β -unsaturated copper(I) carbene **VII** (Scheme 7). As expected, the imaginary frequency of **TS5** is associated with the elongation of the C-Cu bond and the rotation of methylene group corresponding with the re-hybridization sp^3 to sp^2 of the carbon atom.



Scheme 7. Ring-opening of **VI** leading to the formation of copper(I) carbene intermediate **VII**. Lengths and angles are in Å and degrees, respectively.

As the copper(I) carbene **VII** is a key intermediate in the mechanism proposed, an additional study of the potential-energy surface corresponding to the transformation of the π -coordinated complex **Va** into metal carbene **VII**, was carried out at higher levels of theory, namely, B3LYP/6-311+G(d) and

MP2/6-311+G(d) [using the 6-31G(d) basis set for Cu and Br atoms]. These calculations show that the topology of the potential-energy surface for the transformation of **Va** into **VII**, does not change at higher levels of theory: all the stationary points found at the B3LYP/6-31G(d) level were also found to be present in these calculations. Additional details of this study can be found in the ESI section.

Conjugate Addition of Pyridine **1a** to Copper(I) Carbene intermediate.

According to the mechanistic proposal presented in Scheme 2, after the formation of the α,β -unsaturated copper(I) carbene **VII**, the next step is a Michael-type nucleophilic addition of **1a** to **VII**, leading to the Michael adduct **VIII** (Figure 3). **TS6** corresponding to the conjugate addition of **1a** to **VII**, presents an imaginary normal mode associated to the stretching of the forming-breaking bond between N and C atoms, and the rehybridization of the methylene group of the carbene intermediate, **VII**, leading to intermediate **VIIIa**. Also, as expected in an addition of a nucleophile to sp^2 carbon atom, the attack angle is close to the value of the tetrahedral geometry.

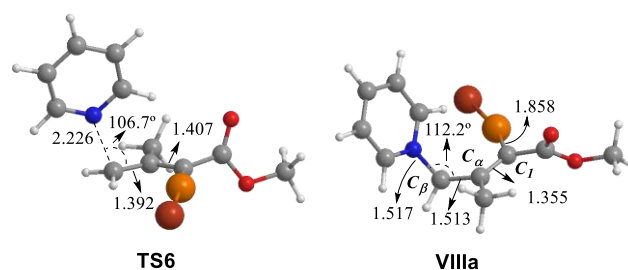


Figure 3. Transition structure (**TS6**) and intermediate **VIIIa** corresponding to the Michael-type addition of **1a** to copper(I) carbene **VII**. Lengths and angles are in Å and degrees, respectively.

In the Michael adduct **VIIIa**, the bond between the nitrogen atom of **1a** and the carbon at termini of **VII** is fully formed and this carbon atom shows a geometry corresponding to the sp^3 hybridization; also, the C_1 - C_α bondlength in **VIIIa** (1.355 Å) decreased, compared with the value (1.445 Å) in **VII**, whereas the C_α - C_β bondlength (1.513 Å) in **VIIIa** is longer than the value (1.360 Å) in carbene **VII**, these changes being in agreement with those expected in a conjugate addition of a nucleophile to an α,β -unsaturated system.

Intramolecular Cyclization and Reductive Elimination of intermediate **VIIIa**: Formation of the Indolizine skeleton, **Xa**.

The Michael adduct **VIIIa** could undergo an intramolecular cyclization through the attack of the copper to the *ortho* position of the pyridine ring, thus forming the metalacyclohexene **IXa** (Figure 4).

The vibrational normal mode associated to the imaginary frequency of **TS7**, corresponds to a rotation around the bond between C_α and C_β carbon atoms, which leads the copper close to the C-2 of the pyridine ring, thus allowing for the formation of the Cu-C bond in intermediate **IXa**.

As a result of the copper addition to the pyridine ring, the N-C bondlength in metalacycle **IXa** (1.395 Å) is increased respect to the value of N-C bondlength (1.339 Å) in **1a**. The bond between copper and carbon atoms in intermediate **IXa**, seems to be dominated by the electrostatic interaction between the electron-deficient carbon at the position 2 in the pyridine ring and the copper-bromide electron-rich moiety. This is reflected in the fact that the value of the H-C-Cu bond angle in **IXa** is about 92°, which means that the hydrogen attached to C2 remains in the plane of the pyridine ring. Also, the metalacyclohexene **IXa** intermediate appears to adopt a pseudo-chair conformation.

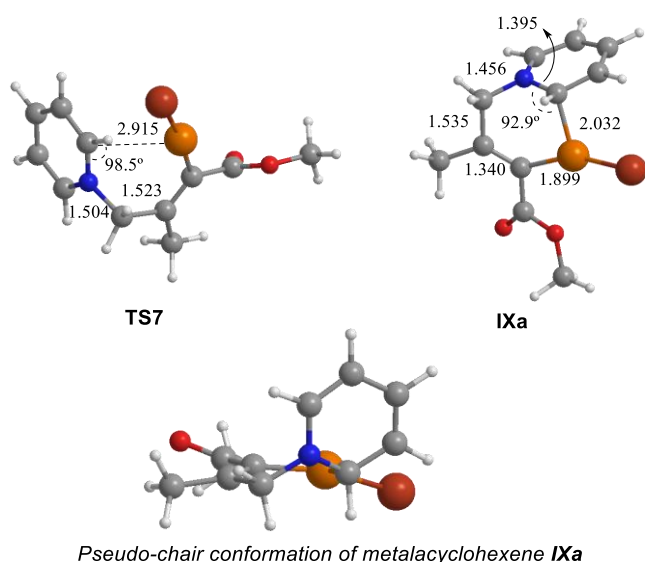
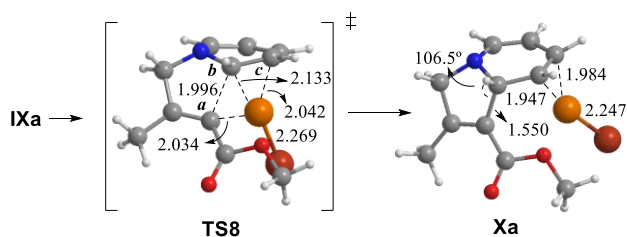


Figure 4. Transition structure **TS7** and metalacyclohexene intermediate, **IXa**, formed in the intramolecular cyclization of intermediate **VIIIa**. Lengths and angles are in Å and degrees, respectively.

The final step of the formation of the indolizine system is the reductive elimination of copper in the metalacyclohexene **IXa**, through transition structure **TS8** (Scheme 8).



Scheme 8. Reductive elimination in metalacyclohexene **IXa** to give rise to the CuBr-complexed indolizine derivative **Xa**. Lengths and angles are in Å and degrees, respectively.

The normal mode associated to the imaginary frequency of **TS8** corresponds to the stretching of the C_σ-C_b bond being formed, the breaking of the C_σ-Cu bond and the formation of the bond between copper and the carbon atom of the ring, C_c. The formation of the C-C bond leads to the indolizine ring **Xa**, which is π-coordinated to copper(I) bromide, and the formal oxidation state of copper changes from Cu(III) to Cu(I).

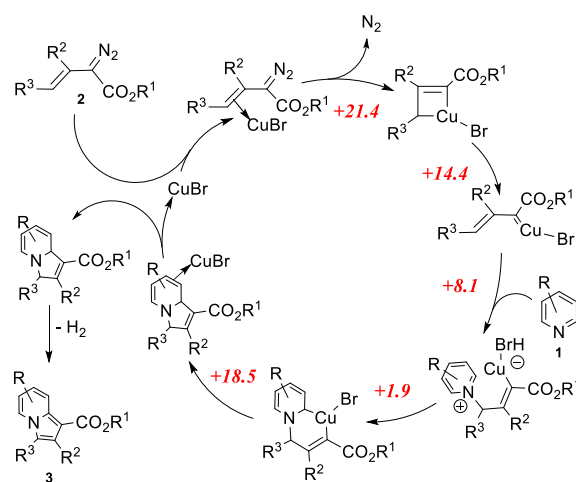
The relative free energies for the stationary points located in this reaction steps are shown in Table 1. It can be seen that, in sharp contrast with the results found in the direct addition mechanism, the values for the activation free-energies for the reaction of **2a** with CuBr to give copper(I) carbene **VII** and the subsequent addition of pyridine **1a** to **VII**, are compatible with the experimental conditions.

Table 1. Relative Gibbs free energies (kcal mol⁻¹) of the stationary points located for the reactions of pyridine derivatives **1a**, **1b** and **1c**.

Reaction of 1a with 2a		Reaction of 1b with 2a		Reaction of 1c with 2a	
Stationary Points	ΔG_{rel}	Stationary Points	ΔG_{rel}	Stationary Points	ΔG_{rel}
1a + VII	0.0	1b + VII	0.0	1c + VII	0.0
TS6_a	8.1	TS6_b	+7.9	TS6_c	+9.6
VIIIa	-1.3	VIIIb	-5.1	VIIIc	+2.9
TS7_a	+1.9	TS7_b-ortho	-3.1	TS7_c-ortho	+7.8
		TS7_b-para	-1.7	TS7_c-para	+4.6
IXa	-13.7	IXb-ortho	-13.3	IXc-ortho	-12.3
		IXb-para	-13.4	IXc-para	-13.7
TS8_a	+18.5	TS8_b-ortho	+4.5	TS8_c-ortho	+11.6
		TS8_b-para	+4.6	TS8_c-para	+2.0
Xa	-17.0	Xb-ortho	-18.5	Xc-ortho	-21.8
		Xb-ortho	-16.4	Xc-ortho	-25.2

Catalytic cycle proposed for the reaction of pyridine derivatives with alkenyldiazoacetates

According to the previously described computational results on the mechanism for the CuBr-catalyzed reaction of pyridine **1a** with diazo compound **2a**, a catalytic cycle could be proposed (Scheme 9).



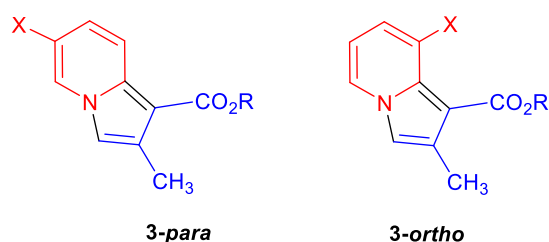
Scheme 9. Catalytic cycle proposed for the reaction of pyridine derivatives **1** with alkenyldiazoacetates **2**, in the presence of copper(I) bromide, to yield indolizine derivatives **3**. The numbers in italics correspond to the ΔG^\ddagger (in kcal mol⁻¹) for the specific case of the reaction of **1a** with **2a**.

The process starts with the formation of a π -coordinated complex between **2** and CuBr, which evolves with dinitrogen extrusion to give a copper(I) carbene intermediate. A conjugate addition of pyridine derivative **1** to the carbene intermediate, leads to a Michael-type adduct which undergoes an intramolecular cyclization to give a metallacyclohexene, which after a reductive elimination regenerates the free catalyst and the Indolizine-type product. The oxidative aromatization of this product gives the final aromatic indolizine derivative **3** (see ESI for details).

As shown in Scheme 9, in the case of the reaction of pyridine **1a** with alkenyldiazoacetate **2a**, the rate-determining step of the cycle is the transformation of the complex formed between diazocompound **2a** and the catalyst, CuBr, into a metallacyclobutene, which leads to the copper carbene intermediate. In addition, the predicted values for the activation free energies of the steps of the catalytic cycle are compatible with the conditions in which these reactions are carried out.

Regioselectivity in the Annulation Reactions of Pyridine derivatives **1b**, **1c**, **1d** and **1e**.

It was found experimentally that the reaction of 3-substituted pyridines with diazocompound **2a**, takes place with partial or total regioselectivity (Figure 5).⁶



	ratio 3-para / 3-ortho
X = CH ₃	1 : 7
X = NO ₂	3-para only
X = CO ₂ CH ₃	3 : 1
X = F	1 : 3

Figure 5. Regioselectivity observed (for R = Et) in the annulation reaction of pyridine derivatives **1b-e**. The *para/ortho* indicators refer to the position of the pyridine ring, 6 or 2, respectively, to participate in the ring-closure step.

In order to determine if the mechanism previously described could account for the experimentally observed regioselectivity, all stationary points of the reaction path of pyridines **1b** and **1c** were located. The relative free-energies of these points are collected in Table 1 (see ESI for full details).

The indolizine ring is formed in the reductive elimination step and in the case of the reaction of 3-substituted pyridines, the regiochemistry could be determined, either by the intramolecular cyclization of the Michael adduct intermediate or by the reductive elimination step, as it is shown in Figure 6. In the case of the reaction of **1b** with diazocompound **2a**, the values of the activation free-energies for the reductive

elimination of intermediates **IXb-ortho** and **IXb-para**, are quite similar (17.8 and 18.0 kcal mol⁻¹, respectively), but in the cyclization step of the Michael adduct **VIIIb** which leads to the *ortho* and *para* metallacycles, **IXb-ortho** and **IXb-para**, these values are, $\Delta G^\ddagger_{(\text{ortho})} = 2.0$ and $\Delta G^\ddagger_{(\text{para})} = 3.4$ kcal mol⁻¹, respectively. According to these differences in ΔG^\ddagger , the ratio **3-para/3-ortho** is predicted to be about 1/7.7, in good agreement with the experimental value.

In the case of the reaction of **2a** with **1c** the computed values of ΔG^\ddagger , for the *ortho* and *para* reaction pathways, namely 15.7 and 23.9 kcal mol⁻¹, respectively, agree very well with the experimentally observed regioselectivity (see Figure 5).

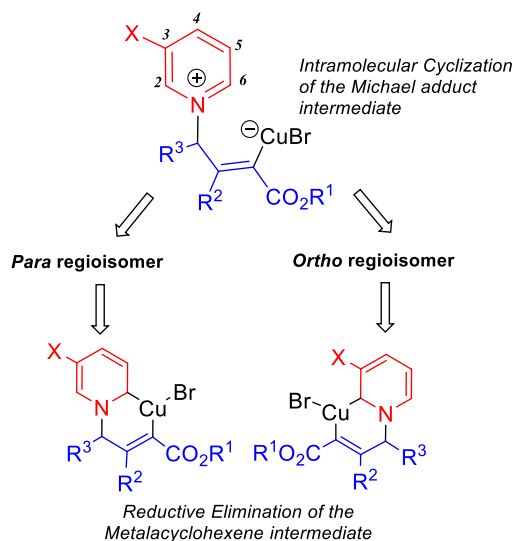


Figure 6. Regiochemistry-determining steps in the CuBr-catalyzed reaction of pyridine derivatives with diazocompounds.

In the cases of the reaction of pyridine derivatives **1d** and **1e** with **2a**, we have not fully explored their corresponding potential energy surface, but only the transition structures for the reductive elimination step were located (see the ESI section). However, the regioselectivity predicted in each case is in agreement with the one show in Figure 5: the *para/ortho* ratios are 7/1 in the case of the reaction of **1d**, and 1/10 for the reaction of **1e**, both values slightly overestimated as compared with the experimental ones.

Conclusions

We have computationally studied the copper(I)-catalyzed [3+2] cycloaddition of vinyldiazo compounds towards pyridine derivatives. The computed mechanism consists of: (a) initial decomposition of the diazo function and generation of a copper carbene intermediate, (b) attack of the pyridine to the vinylogous position of the carbene, (c) a cyclization step to provide a metallacyclohexene intermediate, (d) reductive elimination and (e) oxidative aromatization. This mechanism would satisfactorily account for the subtle regiochemical trends that have been found in the experimental work. In contrast, an alternative pathway involving initial Lewis acid-catalyzed

activation of the pyridine reagent seems to be an unproductive route.

Conflicts of interest

There are no conflicts to declare.

Acknowledgements

The authors received no specific funding for this work.

Notes and references

- Selected reviews on synthetic applications of diazo compounds: M. P. Doyle, M. A. McKerverey and T. Ye, *Modern Catalytic Methods for Organic Synthesis with Diazo Compounds: From Cyclopropanes to Ylides*, Wiley, New York, 1998; M. P. Doyle and D. C. Forbes, *Chem. Rev.*, 1998, **98**, 911; H. M. L. Davies and R. E. J. Beckwith, *Chem. Rev.*, 2003, **103**, 2861; H. M. L. Davies and J. R. Manning, *Nature*, 2008, **451**, 417; Y. Zhang and J. Wang, *Chem. Commun.*, 2009, 5350; M. P. Doyle, R. Duffy, M. Ratnikov and L. Zhou, *Chem. Rev.* 2010, **110**, 704; H. M. L. Davies and Y. Lian, *Acc. Chem. Res.* 2012, **45**, 923; Q. Xiao, Y. Zhang and J. Wang, *Acc. Chem. Res.* 2013, **46**, 236; A. Ford, H. Miel, A. Ring, C. N. Slattery, A. R. Maguire and M. A. McKerverey, *Chem. Rev.* 2015, **115**, 9981.
- For recent reviews on metal-catalyzed transformations of vinyldiazo reagents, see: Q.-Q. Cheng, Y. Mu, J. Yedoyan and M. P. Doyle, *ChemCatChem.*, 2018, **10**, 488; Q.-Q. Cheng, Y. Deng, M. Lankelma and M. P. Doyle, *Chem. Soc. Rev.*, 2017, **46**, 5425; X. Xu and M. P. Doyle, *Acc. Chem. Res.*, 2014, **47**, 1396.
- Representative examples of rhodium-catalyzed transformations of vinyldiazo compounds: Y. Deng, H. Qiu, H. D. Srinivas and M. P. Doyle, *Curr. Org. Chem.* 2016, **20**, 61; Q.-Q. Cheng, M. Lankelma, D. Wherritt, H. Arman and M. P. Doyle, *J. Am. Chem. Soc.*, 2017, **139**, 9839; Q.-Q. Cheng, J. Yedoyan, H. Arman, M. P. Doyle, *Angew. Chem. Int. Ed.*, 2016, **55**, 5573; B. T. Parr and H. M. L. Davies, *Org. Lett.* 2015, **17**, 794; P. E. Guzmán, Y. Lian and H. M. L. Davies, *Angew. Chem. Int. Ed.*, 2014, **53**, 13083; A. G. Smith and H. M. L. Davies, *J. Am. Chem. Soc.* 2012, **134**, 18241; D. Valette, Y. Lian, J. P. Haydek, K. I. Hardcastle and H. M. L. Davies, *Angew. Chem. Int. Ed.*, 2012, **51**, 8636; Y. Lian and H. M. L. Davies, *J. Am. Chem. Soc.*, 2010, **132**, 440;
- For recent reviews on coinage metal catalyzed transformations of diazo compounds, see: E. López, S. González-Pelayo and L. A. López, *Chem. Rec.* 2017, **17**, 312; M. R. Fructos, M. M. Díaz-Requejo and P. J. Pérez, *Chem. Commun.* 2016, **52**, 7326; L. Liu and J. Zhang, *Chem. Soc. Rev.* 2016, **45**, 506; F. Wei, C. Song, Y. Ma, L. Zhou, C.-H. Tung and Z. Xu, *Sci. Bull.* 2015, **60**, 1479.
- Selected gold-catalyzed transformations of vinyldiazo reagents: V. V. Pagar, A. M. Jadhav and R.-S. Liu, *J. Am. Chem. Soc.*, 2011, **133**, 20728; J. Barluenga, G. Lonzi, M. Tomás and L. A. López, *Chem. Eur. J.*, 2013, **19**, 1573; J. F. Briones and H. M. L. Davies, *J. Am. Chem. Soc.*, 2013, **135**, 13314; G. Lonzi and L. A. López, *Adv. Synth. Catal.*, 2013, **355**, 1948; D. Zhang, G. Xu, D. Ding, C. Zhu, J. Li and J. Sun, *Angew. Chem. Int. Ed.*, 2014, **53**, 11070; E. López, G. Lonzi and L. A. López, *Organometallics*, 2014, **33**, 5924; V. V. Pagar and R.-S. Liu, *Angew. Chem. Int. Ed.*, 2015, **54**, 4923; G. Xu, C. Zhu, W. Gu, J. Li and J. Sun, *Angew. Chem. Int. Ed.*, 2015, **54**, 883; C. Zhu, G. Xu and J. Sun, *Angew. Chem. Int. Ed.*, 2016, **55**, 11867; E. López, J. González and L. A. López, *Adv. Synth. Catal.*, 2016, **358**, 1428; E. López, G. Lonzi, J. González and L. A. López, *Chem. Commun.*, 2016, **52**, 9398.
- J. Barluenga, G. Lonzi, L. Riesgo, L. A. López and M. Tomás, *J. Am. Chem. Soc.*, 2010, **132**, 13200.
- M. P. Doyle, M. Yan, W. Hu and L. S. Gronenberg, *J. Am. Chem. Soc.*, 2003, **125**, 4692. In this contribution, the authors also documented a divergent regiochemical outcome for the rhodium-catalyzed reaction. In contrast to the copper-catalyzed reaction, a rhodium carbene complex resulting from initial decomposition of the diazo function was proposed as key intermediate.
- The use of copper catalysts for diazo decomposition has been widely documented. Representative reviews: W. Kirmse, *Angew. Chem. Int. Ed.*, 2003, **42**, 1088; X. Zhao, Y. Zhang, J. Wang, *Chem. Commun.*, 2012, **48**, 10162.
- See, for example: O. N. Faza, R. A. Rodríguez and C. S. López, *Theor. Chem. Acc.* 2011, **128**, 647; E. L. Noey, Y. Luo, L. Zhang and K. N. Houk, *J. Am. Chem. Soc.*, 2012, **134**, 1078; A. Comas-Vives, C. Gonzalez-Arellano, A. Corma, M. Iglesias, F. Sanchez and G. Ujaque, *J. Am. Chem. Soc.*, 2006, **128**, 4756; B. F. Straub, *Chem. Commun.*, 2004, 1726; E. Soriano and J. Marco-Contelles, *Organometallics*, 2006, **25**, 4542; C. Nevado and A. M. Echavarren, *Chem. Eur. J.*, 2005, **11**, 3155.
- M. J. Frisch, G. W. Trucks, H. B. Schlegel, G. E. Scuseria, M. A. Robb, J. R. Cheeseman, J. A. Montgomery, Jr., T. Vreven, K. N. Kudin, J. C. Burant, J. M. Millam, S. S. Iyengar, J. Tomasi, V. Barone, B. Mennucci, M. Cossi, G. Scalmani, N. Rega, G. A. Petersson, H. Nakatsuji, M. Hada, M. Ehara, K. Toyota, R. Fukuda, J. Hasegawa, M. Ishida, T. Nakajima, Y. Honda, O. Kitao, H. Nakai, M. Klene, X. Li, J. E. Knox, H. P. Hratchian, J. B. Cross, C. Adamo, J. Jaramillo, R. Gomperts, R. E. Stratmann, O. Yazyev, A. J. Austin, R. Cammi, C. Pomelli, J. W. Ochterski, P. Y. Ayala, K. Morokuma, G. A. Voth, P. Salvador, J. J. Dannenberg, V. G. Zakrzewski, S. Dapprich, A. D. Daniels, M. C. Strain, O. Farkas, D. K. Malick, A. D. Rabuck, K. Raghavachari, J. B. Foresman, J. V. Ortiz, Q. Cui, A. G. Baboul, S. Clifford, J. Cioslowski, B. B. Stefanov, G. Liu, A. Liashenko, P. Piskorz, I. Komaromi, R. L. Martin, D. J. Fox, T. Keith, M. A. Al-Laham, C. Y. Peng, A. Nanayakkara, M. Challacombe, P. M. W. Gill, B. Johnson, W. Chen, M. W. Wong, C. Gonzalez, and J. A. Pople; Gaussian 03, Revision C.02, Gaussian, Inc., Wallingford CT, 2004.; M. J. Frisch, G. W. Trucks, H. B. Schlegel, G. E. Scuseria, M. A. Robb, J. R. Cheeseman, G. Scalmani, V. Barone, B. Mennucci, G. A. Petersson, H. Nakatsuji, M. Caricato, X. Li, H. P. Hratchian, A. F. Izmaylov, J. Bloino, G. Zheng, J. L. Sonnenberg, M. Hada, M. Ehara, K. Toyota, R. Fukuda, J. Hasegawa, M. Ishida, T. Nakajima, Y. Honda, O. Kitao, H. Nakai, T. Vreven, J. A. Montgomery, Jr., J. E. Peralta, F. Ogliaro, M. Bearpark, J. J. Heyd, E. Brothers, K. N. Kudin, V. N. Staroverov, T. Keith, R. Kobayashi, J. Normand, K. Raghavachari, A. Rendell, J. C. Burant, S. S. Iyengar, J. Tomasi, M. Cossi, N. Rega, J. M. Millam, M. Klene, J. E. Knox, J. B. Cross, V. Bakken, C. Adamo, J. Jaramillo, R. Gomperts, R. E. Stratmann, O. Yazyev, A. J. Austin, R. Cammi, C. Pomelli, J. W. Ochterski, R. L. Martin, K. Morokuma, V. G. Zakrzewski, G. A. Voth, P. Salvador, J. J. Dannenberg, S. Dapprich, A. D. Daniels, O. Farkas, J. B. Foresman, J. V. Ortiz, J. Cioslowski, and D. J. Fox; Gaussian 09, Revision B.01, Gaussian, Inc., Wallingford CT, 2009.